THE JOURNAL OF BIOLOGICAL CHEMISTRY VOL. 281, NO. 2, pp. 723–732, January 13, 2006

Functional Characterization of Dehydratase/Aminotransferase Pairs from *Helicobacter* and *Campylobacter*

ENZYMES DISTINGUISHING THE PSEUDAMINIC ACID AND BACILLOSAMINE BIOSYNTHETIC PATHWAYS[*][S]

Received for publication, October 11, 2005, and in revised form, November 10, 2005 Published, JBC Papers in Press, November 11, 2005, DOI 10.1074/jbc.M511021200

Ian C. Schoenhofen, David J. McNally, Evgeny Vinogradov, Dennis Whitfield, N. Martin Young, Scott Dick, Warren W. Wakarchuk, Jean-Robert Brisson, and Susan M. Logan[1]

From the Institute for Biological Sciences, National Research Council, Ottawa, Ontario K1A OR6, Canada

Helicobacter pylori **and** ***Campylobacter jejuni*** **have been shown to modify their flagellins with pseudaminic acid (Pse), via *O*-linkage, while *C. jejuni* also possesses a general protein glycosylation pathway (Pgl) responsible for the *N*-linked modification of at least 30 proteins with a heptasaccharide containing 2,4-diacetamido-2,4,6-trideoxy-α-D-glucopyranose, a derivative of bacillosamine. To further define the Pse and bacillosamine biosynthetic pathways, we have undertaken functional characterization of UDP-α-D-GlcNAc modifying dehydratase/aminotransferase pairs, in particular the *H. pylori* and *C. jejuni* flagellar pairs HP0840/HP0366 and Cj1293/Cj1294, as well as the *C. jejuni* Pgl pair Cj1120c/Cj1121c using His_6-tagged purified derivatives. The metabolites produced by these enzymes were identified using NMR spectroscopy at 500 and/or 600 MHz with a cryogenically cooled probe for optimal sensitivity. The metabolites of Cj1293 (PseB) and HP0840 (FlaA1) were found to be labile and could only be characterized by NMR analysis directly in aqueous reaction buffer. The Cj1293 and HP0840 enzymes exhibited C6 dehydratase as well as a newly identified C5 epimerase activity that resulted in the production of both UDP-2-acetamido-2,6-dideoxy-β-L-*arabino*-4-hexulose and UDP-2-acetamido-2,6-dideoxy-α-D-*xylo*-4-hexulose. In contrast, the Pgl dehydratase Cj1120c (PglF) was found to possess only C6 dehydratase activity generating UDP-2-acetamido-2,6-dideoxy-α-D-*xylo*-4-hexulose. Substrate-specificity studies demonstrated that the flagellar aminotransferases HP0366 and Cj1294 utilize only UDP-2-acetamido-2,6-dideoxy-β-L-*arabino*-4-hexulose as substrate producing UDP-4-amino-4,6-dideoxy-β-L-AltNAc, a precursor in the Pse biosynthetic pathway. In contrast, the Pgl aminotransferase Cj1121c (PglE) utilizes only UDP-2-acetamido-2,6-dideoxy-α-D-*xylo*-4-hexulose producing UDP-4-amino-4,6-dideoxy-α-D-GlcNAc (UDP-2-acetamido-4-amino-2,4,6-trideoxy-α-D-glucopyranose), a precursor used in the production of the Pgl glycan component 2,4-diacetamido-2,4,6-trideoxy-α-D-glucopyranose.**

Campylobacter jejuni, a principle cause of acute gastroenteritis, and *Helicobacter pylori*, a major etiological agent of gastroduodenal disease, are microaerophilic Gram-negative bacteria (1, 2). As these organisms have significant medical and public health importance, recent genomic efforts have resulted in the complete sequencing of at least two genomes for each organism with others in progress (3–6). The sequencing of *C. jejuni* genomes revealed an unusual plethora (>8%) of glycan biosynthetic genes dedicated to surface carbohydrate biosynthesis, as well as significant diversity of glycan biosynthetic gene content among individual strains (7). These gene products appear to be involved in the biosynthesis of the glycoconjugate structures lipooligosaccharide and capsular polysaccharide, as well as in the biosynthesis of the novel glycans utilized by the *N*- and *O*-linked protein glycosylation systems. Each respective glycoconjugate structure is represented by a distinct and dedicated genetic locus (lipooligosaccharide Cj1131-Cj1152, capsule Cj1448c-Cj1413c, *N*-linked glycan Cj1119-Cj1130, *O*-linked glycan Cj1293-Cj1342). Although much progress has been made toward biosynthetic and structural characterization of lipooligosaccharide, capsular polysaccharide, and *N*-linked systems, the biochemical characterization of the *O*-linked system is currently less well defined (7–9).

C. jejuni has been shown to modify its flagellin with the novel nine-carbon sialic acid-like sugar 5,7-diacetamido-3,5,7,9-tetradeoxy-L-*glycero*-L-*manno*-nonulosonic acid or pseudaminic acid (Pse),[2] as well as related derivatives, via *O*-linkage at up to 19 sites/monomer (10, 11). The modification of flagellin appears to be important for flagellar assembly, as mutations in putative *O*-linked glycosylation genes result in non-motile cells lacking flagella (11). *C. jejuni* also possesses a general protein glycosylation pathway (Pgl) that is responsible for the *N*-linked addition of a heptasaccharide containing *N*-acetylgalactosamine, glucose, and 2,4-diacetamido-2,4,6-trideoxy-α-D-glucopyranose (2,4-diacetamido-Bac) to at least 30 different proteins (12, 13). Interruption of either the flagellin glycosylation or Pgl pathway results in loss of colonization and, hence, virulence (14, 15); as such, the Pse and Bac biosynthetic pathways offer potential as novel therapeutic targets. Although biosynthesis of both the complex carbohydrates Bac and Pse from the initial *N*-acetyl-hexosamine building block, UDP-α-D-GlcNAc, would involve the actions of a sugar-nucleotide dehydratase and its corresponding aminotransferase, the precise biosynthetic steps that distinguish these pathways are currently unknown.

* This study was supported by the National Research Council Genomics and Health Initiative. The costs of publication of this article were defrayed in part by the payment of page charges. This article must therefore be hereby marked "*advertisement*" in accordance with 18 U.S.C. Section 1734 solely to indicate this fact.

[S] The on-line version of this article (available at http://www.jbc.org) contains supplemental Figs. S1–S5 and supplemental Tables S1 and S2.

[1] To whom correspondence should be addressed. Tel.: 613-990-0839; Fax: 613-952-9092; E-mail: susan.logan@nrc-cnrc.gc.ca.

[2] The abbreviations used are: Pse, 5,7-diacetamido-3,5,7,9-tetradeoxy-L-*glycero*-L-*manno*-nonulosonic acid (also known as pseudaminic acid); AltNAc, *N*-acetyl-β-L-altrosamine; Bac, 2,4-diamino-2,4,6-trideoxy-α-D-glucopyranose (also known as bacillosamine); CE, capillary electrophoresis; δ, chemical shift; HMBC, heteronuclear multiple bond coherence; HSQC, heteronuclear single quantum coherence; *J*, proton-coupling constant; NOE, nuclear Overhauser effect; NOESY, nuclear Overhauser effect spectroscopy; Pgl, general protein glycosylation pathway; PLP, pyridoxal phosphate; TOCSY, total correlation spectroscopy.

TABLE 1
Plasmids used in this study

Plasmid	Description	Source/Reference
pCR2.1	Ap^r, Kn^r, oriColE1, *lac* promoter, used for TA cloning	Invitrogen
pET30a	Kn^r, oriColE1, T7 promoter, used for C-terminal His_6-tagged protein expression	Novagen
pFO4	pET15b derivative; Ap^r, oriColE1, T7 promoter, used for N-terminal His_6-tagged protein expression	This study
pNRC8.1	*HP0840* NdeI-XhoI in pET30a, encodes for $HP0840His_6$	This study
pNRC37.1	*HP0366* BamHI-EcoRI in pFO4, encodes for $His_6HP0366$	This study
pNRC20.3	*Cj1293* NdeI-XhoI in pET30a, encodes for $Cj1293His_6$	This study
pNRC82.1	*Cj1294* BamHI-EcoRI in pFO4, encodes for $His_6Cj1294$	This study
pNRC40.1	Truncated *Cj1120C* BamHI-EcoRI in pFO4, encodes for $His_6SFCj1120c$	This study
pNRC41.3	*Cj1121c* BamHI-EcoRI in pFO4, encodes for $His_6Cj1121c$	This study

The flagellins of *H. pylori* have also been shown to be modified with Pse, where glycosylation again appears to be required for assembly of a functional filament (16). Homologs of *Campylobacter* flagellar glycosylation components are present in both the *H. pylori* 26695 and the J99 genomes (5, 6). Metabolomic analysis of various *O*-linked glycan biosynthetic mutants revealed an accumulation of biosynthetic intermediates and loss of CMP-Pse, thus confirming a role for these gene products in the Pse biosynthetic pathway, although the precise enzymatic steps of this pathway remain ill defined (16). To unequivocally define the Bac and Pse biosynthetic pathways, we have undertaken functional characterization of the *C. jejuni* and *H. pylori* flagellar pairs Cj1293/Cj1294 and HP0840/HP0366, as well as the *C. jejuni* Pgl pair Cj1120c/Cj1121c, using His_6-tagged recombinant proteins. These results convincingly demonstrate that the Pse and Bac biosynthetic pathways are discrete, incorporating unique and distinct dehydratase/aminotransferase pairs, and explain the clear phenotypic differences observed between isogenic mutants from the two pathways.

EXPERIMENTAL PROCEDURES

DNA Techniques and Plasmid Construction—Plasmid DNA minipreparations and agarose gel purification of DNA fragments were performed using Qiagen's QIAprep spin kit and QIAquick gel extraction kit, respectively. All other recombinant DNA methods and analyses were performed as described by Sambrook *et al.* (17). Vector or recombinant plasmids were transformed by electroporation into electrocompetent Top10F′ or DH10B (Invitrogen) *Escherichia coli* cells for cloning purposes or BL21[DE3] (Novagen, Madison, WI) *E. coli* cells for protein production. The polymerase chain reaction (PCR) was used to amplify *H. pylori* 26695 DNA or *C. jejuni* 11168 DNA for subsequent cloning. A list of cloning vectors and recombinant plasmids is provided in Table 1, and pertinent oligos are provided in Table 2. PCR was performed in a 50-μl reaction containing 10 mM Tris, pH 8.3, 50 mM KCl, 1.5 mM $MgCl_2$, dNTPs at a final concentration of 200 μM, 0.2 μM of each primer, and 2.5 units of *Taq* DNA polymerase (Roche Applied Science). Amplicons were ligated with pCR2.1 and the agarose-purified restriction fragments were then ligated with either pET30a or pFO4 (a pET15b (Novagen) derivative in which the EcoRI-HindIII sites have been removed and replaced by sequence encoding MGSSHHHHHH). pET30a and pFO4 recombinant plasmids were sequenced using both forward and reverse T7 primers, as well as NRC175 and NRC160, respectively. Plasmid pNRC8.1 encodes a C-terminal His_6-tagged derivative of HP0840 or FlaA1; pNRC37.1 encodes an N-terminal His_6-tagged derivative of HP0366; pNRC20.3 encodes a C-terminal His_6-tagged derivative of Cj1293 or PseB; pNRC82.1 encodes an N-terminal His_6-tagged derivative of Cj1294; pNRC40.1 encodes an N-terminal His_6-tagged soluble derivative of Cj1120c or PglF (residues 130–590); and pNRC41.3 encodes an N-terminal His_6-tagged derivative of Cj1121c or PglE.

His_6-tagged Protein Purification—For functional characterization and for the isolation of enzyme products, each expression strain was grown in 500 ml of 2x yeast tryptone (17) with either kanamycin (50 μg ml^{-1}) or ampicillin (50 μg ml^{-1}) for selection. The cultures were grown at 30 °C, induced at an OD_{600} of 0.6 with 0.1 mM isopropyl-1-thio-β-D-galactopyranoside, and harvested 2.75 h later. Cell pellets were resuspended in lysis buffer (50 mM sodium phosphate, pH 7.7, 400 mM NaCl, 10 mM β-mercaptoethanol) containing 10 mM imidazole and complete protease inhibitor mixture, EDTA-free (Roche Applied Science). After addition of 10 μg ml^{-1} of RNaseA and DNaseI (Roche Applied Science), the cells were disrupted by two passes through an emulsiflex C5 (20,000 psi). Lysates were centrifuged at 100,000 × *g* for 1 h at 4 °C, and the supernatant fraction was applied to a 1-ml nickel-nitrilotriacetic acid (Qiagen) column equilibrated in 10 mM imidazole lysis buffer, using a flow rate of 0.5 ml min^{-1}. After sample application, the column was washed with 20 column volumes of 10 mM imidazole Lysis buffer. To elute the protein of interest, a linear gradient from 10 to 100 mM imidazole, in lysis buffer, over 60 column volumes was applied to the column prior to a final pulse of 40 column volumes of 200 mM imidazole lysis buffer. Fractions containing the purified protein of interest, as determined by SDS-PAGE (12.5%) and Coomassie staining, were pooled and dialyzed against dialysis buffer (25 mM sodium phosphate, pH 7.7, 50 mM NaCl) overnight at 4 °C. Protein concentration was measured spectrophotometrically using A_{280} 0.1% values ($HP0840His_6$, 0.536; $His_6HP0366$, 0.386; $Cj1293His_6$, 0.669; $His_6Cj1294$, 0.635; $His_6SFCj1120c$, 0.410; $His_6Cj1121c$, 0.902).

Enzymatic Reactions—Purification and dialysis/assay buffers for flagellar glycosylation enzymes were pH 7.2, whereas those for Pgl enzymes were pH 7.7. $HP0840His_6$, $Cj1293His_6$, and $His_6SFCj1120c$ reactions were scaled up to a total reaction volume of 20 ml containing 6 mg of enzyme in the presence of 1 mM UDP-α-D-GlcNAc. Time course samples were also taken for these dehydratase reactions at the times indicated; the samples were then boiled for 3 min, centrifuged for 3 min, and diluted 1:4 in H_2O prior to capillary electrophoresis (CE) analysis. For the $HP0840His_6$/$His_6HP0366$ and the $Cj1293His_6$/$His_6Cj1294$ coupled assays, the reactions were scaled up to a total volume of 30 ml containing 9 mg of each enzyme in the presence of 1 mM UDP-α-D-GlcNAc, 10 mM L-Glu, and 1 mM pyridoxal phosphate (PLP) (the latter two being cofactors necessary for the aminotransfer reaction). To prepare the $His_6Cj1121c$ product, 25 ml of a $His_6SFCj1120c$ reaction containing 7.5 mg of enzyme in the presence of 1 mM UDP-α-D-GlcNAc was allowed to proceed for 210 min. After passage through an Amicon Ultra-15 (10,000 molecular weight cut-off) filter membrane, 6.3 mg of $His_6Cj1121c$ was added to the filtrate, along with PLP and L-Glu, to a final concentration of 1 and 10 mM, respectively. After incubation at 37 °C for 210 min, all reaction mixtures were passed through filter membranes as described above. The filtrates were then either 1) lyophilized and desalted using a Bio-Gel P-2 (Bio-Rad) column in 50 mM ammonium bicarbonate, pH 7.8, as well as a Sephadex G-15 column in pyridine:acetic acid:H_2O (1:2.5:250) prior to NMR, or 2) analyzed directly by NMR in aqueous reaction buffer. Sample composition (*i.e.*

TABLE 2
Oligonucleotides used in this study

Oligonucleotide	Sequence (5′ → 3′)	Purpose
NRC21	CATATGCCAAATCATCAAAACATGCTAGAC	Cloning of pNRC8.1
NRC22	CTCGAGTAATAATTTCAACAAATCATCAGGCTC	
NRC60	GGATCCATGAAAGAGTTTGCTTATAG	Cloning of pNRC37.1
NRC61	AAAGAATTCTCATTCTATTTTAAAACTCTCAAAAG	
NRC43	CATATGTTTAACAAAAAAAATATCTTAATCACGG	Cloning of pNRC20.3
NRC44	CTCGAGAAAACCTTCAGTATGATTGATGATTTC	
NRC137	GGATCCATGCTTACTTATTCTCATCAAAACATC	Cloning of pNRC82.1
NRC138	GAATTCTTATCCACAATATCCCTTTTTAACTTTTTC	
NRC81	GGATCCATGCTTGTGGATTTTAAACCTTC	Cloning of pNRC40.1
NRC74	GAATTCTTATACACCTTCTTTATTGTGTTTAAATTC	
NRC75	GGATCCATGAGATTTTTTCTTTCTCCTCCG	Cloning of pNRC41.3
NRC76	GAATTCTTAAGCCTTTATGCTCTTTAAGATC	
T7-F	TAATACGACTCACTATAGGG	Sequencing of pET30a constructs
T7-R	GCTAGTTATTGCTCAGCGG	
NRC175	TTAATACGACTCACTATAGGGGAATTG	Sequencing of pFO4 constructs
NRC160	GGTTATGCTAGTTATTGCTCAGCGG	

distribution of products II-V, see Fig. 4) was analyzed by CE prior to NMR analysis.

Analysis of Enzymatic Reaction Products by NMR Spectroscopy—Purified reaction products were suspended in 200 μl of 99% deuterated water (Cambridge Isotopes Laboratories Inc.). For examination of metabolites immediately after an enzymatic reaction was completed, the sample (90% H_2O/10% deuterated water) was prepared by adding 20 μl of 99% deuterated water to 180 μl of reaction mixture. All samples were placed into 3-mm NMR tubes. Standard homo- and heteronuclear-correlated two-dimensional ^1H NMR, ^{31}P NMR, ^{13}C HSQC, ^{31}P HSQC, HMBC, COSY, TOCSY, NOESY pulse sequences from Varian (Varian, Palo Alto, CA) were used for general assignments. Selective one-dimensional TOCSY, with a Z-filter, and NOESY experiments were used for complete residue assignment and measurement of proton-coupling constants, $J_{H,H}$, and NOEs (18, 19). The analysis of $J_{H,H}$, and NOE values for various pyranose chair forms was based on the coordinates for ideal pyranose chair conformations (20). NMR experiments were performed with a Varian 600 MHz (^1H) spectrometer equipped with a Varian 5-mm Z-gradient triple resonance (^1H, ^{13}C, ^{15}N) cryogenically cooled probe (cold probe) and with a Varian Inova 500 MHz (^1H) spectrometer with a Varian Z-gradient 3-mm triple resonance (^1H, ^{13}C, ^{31}P) probe. Direct detected ^{31}P NMR spectra were acquired using a Varian Mercury 200 MHz (^1H) spectrometer with a Nalorac 5-mm four nuclei probe. NMR experiments were typically performed at 25 °C with suppression of the H_2O or deuterated HOD resonance at 4.78 ppm. For proton and carbon experiments, the methyl resonance of acetone was used as an internal reference (δ_H 2.225 ppm and δ_C 31.07 ppm), and an external 85% phosphoric acid standard (δ_P 0 ppm) was used to reference ^{31}P spectra.

Analysis of Reaction Products by CE—CE analysis was performed using a P/ACE 5510 system (Beckman Instruments) with diode array detection. The running buffer was 25 mM sodium tetraborate, pH 9.4. The capillary was either bare silica 50 μm × 50 cm or 75 μm × 50 cm, with a detector at 50 cm. The capillary was conditioned before each run by washing with 0.2 M NaOH for 2 min, water for 2 min, and running buffer for 2 min. Samples were introduced by pressure injection for 6–10 s, and the separation was performed at 18 kV for 20 min. Peak integration was done using the Beckman P/ACE station software.

Kinetic Measurements of His_6Cj1294 and His_6Cj1121c—The substrates for the aminotransferases, UDP-2-acetamido-2,6-dideoxy-β-L-*arabino*-4-hexulose or UDP-2-acetamido-2,6-dideoxy-α-D-*xylo*-4-hexulose, were prepared by incubating UDP-α-D-GlcNAc with Cj1293His_6. This substrate preparation was used because of its versatility in studying both Pse and Bac aminotransferases. To determine the preferred substrate for His_6Cj1294 and His_6Cj1121c, ~15 μg of each enzyme was incubated with this Cj1293His_6 filtrate, containing 10 mM L-Glu and 1 mM PLP, and subjected to time course analysis (see above). For kinetic analyses, 5 μg of His_6Cj1294 in a total volume of 200 μl, or 0.15 μg of His_6Cj1121c in a total volume of 400 μl, was incubated at 37 °C in dialysis buffer, pH 7.2, containing 1 mM PLP, 10 mM L-Glu, and various quantities of UDP-2-acetamido-2,6-dideoxy-β-L-*arabino*-4-hexulose and UDP-2-acetamido-2,6-dideoxy-α-D-*xylo*-4-hexulose. His_6Cj1121c assays also contained 40 μg of acetylated bovine serum albumin as carrier protein. Substrate conversion was determined using the molar extinction coefficient of UDP (ϵ_{260} = 10,000). Kinetic constants were calculated using Eadie-Hofstee plots with the program GraphPad Prism 3.

RESULTS

Protein Expression and Purification—In this study, *C. jejuni* protein-coding sequences were cloned from *C. jejuni* 11168 DNA, and *H. pylori* sequences were cloned from strain 26695. Sugar nucleotide-modifying dehydratases were sensitive to N-terminal modification, whereas derivatives containing His_6 tags located at the C terminus exhibited greater stability and solubility compared with their N-terminal counterparts (data not shown). As such, Cj1293 and its functional homolog HP0840 from *H. pylori* were both constructed with C-terminal His_6 tags. In contrast, the Cj1120c derivative was designed with an N-terminal His_6 tag, although, as described below, this was not adjacent to the catalytic domain. This derivative is a soluble truncated version of the native Cj1120c membrane protein, encoding only residues 130–590. From sequence alignment with the short soluble family of dehydratases the Cj1120c polypeptide can be divided into three domains: an N-terminal membrane domain containing four putative transmembrane regions, residues 1–129; a linker region, residues 130–267; and a functional or catalytic domain, residues 268–590 (data not shown). To assess the function of Cj1120c under native state conditions, the linker region was retained, although a construct containing only residues 189–590 exhibited similar activity to that observed with the 130–590 construct (data not shown). In contrast to the dehydratases, the aminotransferases HP0366, Cj1294, and Cj1121c were more resistant to N-terminal modification, but soluble yields were lower compared with the dehydratases (data not shown).

Overall, yields of ~20 mg/liter starting culture were obtained for all of the proteins tested, which had near homogeneity purity (Fig. 1). Protein production levels, as well as the correlation between size estimates determined by SDS-PAGE and that predicted from sequence, confirmed the identity of each purified His_6-tagged protein.

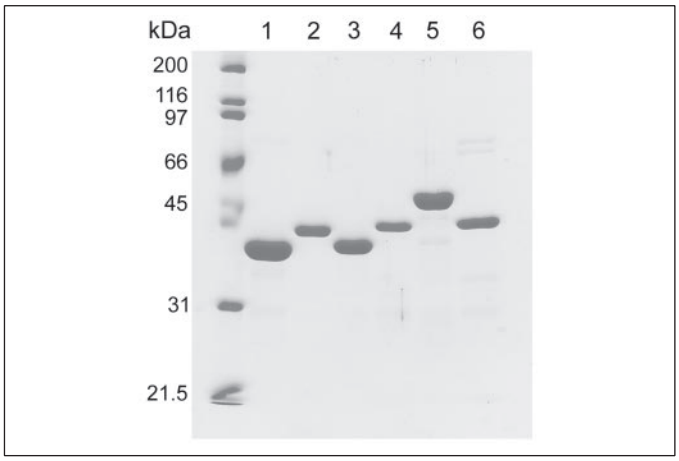

FIGURE 1. **SDS-PAGE (12.5%) analyses of dehydratase/aminotranferase pairs from *H. pylori* 26695 and *C. jejuni* 11168 after nickel-nitrilotriacetic acid purification.** *Lane 1*, HP0840His$_6$; *lane 2*, His$_6$HP0366; *lane 3*, Cj1293His$_6$; *lane 4*, His$_6$Cj1294; *lane 5*, His$_6$SFCj1120c; *lane 6*, His$_6$Cj1121c. Molecular mass standards are shown on the left in kDa.

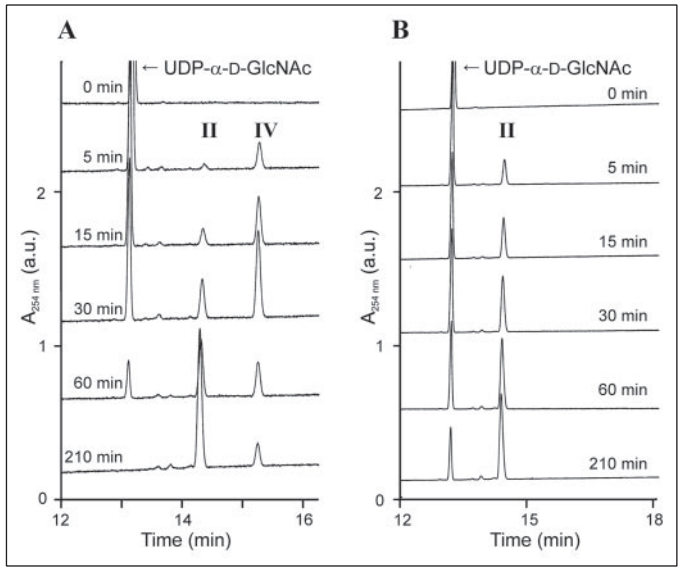

FIGURE 2. **Time course analysis of reaction products obtained after catalysis of UDP-α-D-GlcNAc by Cj1293His$_6$ (*A*) or His$_6$SFCj1120c (*B*).** Reactions were performed at 37 °C using 1 mM UDP-α-D-GlcNAc and 0.3 mg ml^{-1} final enzyme concentration for the various times indicated, after which samples were subjected to capillary electrophoresis. *II* and *IV*, reaction products. *a.u.*, arbitrary units.

CE Characterization of HP0840, Cj1293, and Cj1120c Dehydratase Products—Similar to previously published reports of HP0840 (FlaA1) and Cj1293 (derived from *C. jejuni* subspecies *doylei* ATCC 49349) (21, 22), we found that *11168* Cj1293His$_6$ generated two products in sequential manner by CE. After ~30 min of incubation of Cj1293His$_6$ with UDP-α-D-GlcNAc the predominant product was peak IV (Fig. 2*A*), after which a shift occurred so that at 210 min the prominent product was peak II. In contrast, over the same time course, the only UDP-α-D-GlcNAc reaction product observed with His$_6$SFCj1120c was peak II, which gradually increased over time (Fig. 2*B*). This is similar to the results obtained with WbpM, also a member of the large membrane-bound family of dehydratases (23). Interestingly, there was a greater amount of the breakdown indicator, UDP, present in Cj1293 and HP0840 reactions compared with that observed with the Cj1120c reactions, suggesting that compound IV is less stable than the compound II (data not shown). Moreover, as seen with *49349* Cj1293, the dehydratases studied here did not require the addition of exogenous cofactor NAD(P)$^+$, suggesting that the cofactor was already tightly bound within the enzymes and was recycled throughout catalysis.

NMR Identification of the Products of Cj1120c and Cj1293/HP0840—Based on the results of one- and two-dimensional homo- and heteronuclear NMR experiments, the purified product of Cj1120c (II) was unambiguously identified as UDP-2-acetamido-2,6-dideoxy-α-D-*xylo*-4-hexulose or UDP-*xylo*-sugar. The ^{13}C and ^{1}H chemical shifts, as well as the proton-coupling constants determined for product II (Table 3), were identical to those previously reported for UDP-*xylo*-sugar (24) (supplemental Fig. S1).

Analysis of the reaction of Cj1293 (Fig. 2) and HP0840 (data not shown) by CE revealed that these enzymes produce two products. Because the kinetically slower product that was generated had the same retention time as the product of Cj1120c (data not shown), it was proposed that Cj1293 and HP0840 also produce the UDP-*xylo*-sugar (II). Preliminary attempts to purify and identify the kinetically faster product made by Cj1293 and HP0840 (IV) with NMR were unsuccessful because of the labile nature of this metabolite, which readily degraded during lyophilization (data not shown). To unambiguously identify product IV and confirm the presence of the UDP-*xylo*-sugar (II), the reaction products of Cj1293 and HP0840 were analyzed by NMR immediately following cessation of the reaction at various time points (30 min and 3 h). The slower reaction product formed by both enzymes is the UDP-*xylo*-sugar (II), whereas the initial product formed is UDP-2-acetamido-2,6-dideoxy-β-L-*arabino*-4-hexulose or UDP-*arabino*-sugar (IV) (Fig. 3 and supplemental Fig. S2). Both metabolites could clearly be distinguished in the ^{1}H and ^{13}C HSQC spectrum (Fig. 3, *a and f*). The selective TOCSY of IV H-1 permitted the assignment of H-2 and H-3 (Fig. 3*b*), and the selective TOCSY for H-6 facilitated the assignment of H-5 (data not shown). Accurate proton-coupling constants were measured from the TOCSY spectra (Table 3). The selective NOESY of IV H-1 revealed NOEs to H-2 and H-5 (Fig. 3*c*), whereas the selective NOESY of IV H-6 showed NOEs to H-3 and H-5 (Fig. 3*d*). The proton-coupling constants and NOEs were indicative of an *arabino*-4-hexulose sugar (see below) (supplemental Table S2). The ^{13}C chemical shifts were obtained from the HSQC spectrum (Fig. 3*f*). The proton-coupling constants and NOEs indicated the sugar ring was flexible. The ^{31}P HSQC spectrum and assignments for uridine and ribose confirmed that these were UDP sugars. The use of the cold probe facilitated the assignment of carbon chemical shifts for the highly unstable UDP-*arabino*-sugar as the ^{13}C HSQC spectrum was obtained in a few hours (Fig. 3*f*). HMBC spectra (data not shown) were also obtained within a comparatively short time span using the cold probe and were pivotal in assigning the quaternary C-4 carbons for both II and IV.

CE Characterization of HP0366, Cj1294, and Cj1121c Aminotransferase Products—CE was used to classify the reaction products generated by the dehydratases and aminotransferases as belonging to either the Pse or Bac biosynthetic pathways (Fig. 4). Here, it is shown that the Pse dehydratases HP0840 and Cj1293, as well as the Bac dehydratase Cj1120c, produce the UDP-2-acetamido-2,6-dideoxy-α-D-*xylo*-4-hexulose intermediate after 3.5 h. It should be noted, however, that the initial product of the Pse dehydratases is UDP-2-acetamido-2,6-dideoxy-β-L-*arabino*-4-hexulose. In the coupled reaction, the product of Cj1293His$_6$/His$_6$Cj1294 displayed similar CE mobility compared with the HP0840His$_6$/His$_6$HP0366 product (Fig. 4, *lines E* and *F, peak V*) and migrated faster than all of the compounds we tested by CE. A unique product was noticeable from CE analysis of a sequential His$_6$SFCj1120c/His$_6$Cj1121c reaction as described under "Experimental Procedures," which migrated slightly faster than the control compound

TABLE 3

NMR chemical shifts δ (ppm) and coupling constants *J* (Hz) for metabolites of the bacillosamine and pseudaminic acid biosynthetic pathways

Carbon and proton chemical shifts were referenced to an internal acetone standard (δ_H 2.225 ppm, δ_C 31.07 ppm).

Compound		^{1}H and ^{13}C chemical shifts δ (ppm) and proton coupling constants *J* (Hz)						
		H-1 C-1 $J_{(1,2)}$	H-2 C-2 $J_{(2,3)}$	H-3 C-3 $J_{(3,4)}$	H-4 C-4 $J_{(4,5)}$	H-5 C-5 $J_{(5,6)}$	H-6 C-6	Nac CH_3
UDP-α-D-GlcNAc (I)	δ_H	5.51	3.99	3.81	3.55	3.92	3.82/3.86	2.08
	δ_C	95.1	54.5	71.7	70.3	73.8	61.2	22.9
	$^3J_{H,H}$	3.3	10.2	10.2	10.1			
	$^3J_{H,P(\beta)}$	7.3						
UDP-α-D-*Xylo*-sugar (II)	δ_H	5.45	4.10	3.82		4.12	1.24	2.07
	δ_C	94.9	53.3	72.3	94.3	70.7	12.5	23.0
	$^3J_{H,H}$	3.4	10.8			6.5		
	$^3J_{H,P(\beta)}$	7.0						
UDP-α-D-Bac (III)	δ_H	5.50	4.11	3.94	3.11	4.31	1.38	2.07
	δ_C	95.0	54.6	67.9	58.0	66.6	17.6	22.8
	$^3J_{H,H}$	3.5	10.1	10.2	10.2	6.3		
	$^3J_{H,P(\beta)}$	7.0						
UDP-β-L-*Arabino*-sugar (IV)	δ_H	5.55	4.24	3.92		4.06	1.37	2.07
	δ_C	95.1	53.5	70.0	94.2	76.6	16.5	23.0
	$^3J_{H,H}$	3.1	7.6			7.1		
	$^3J_{H,P(\beta)}$	8.4						
UDP-6-deoxy-β-L-AltNAc4N (V)	δ_H	5.67	4.20	4.30	3.43	4.23	1.43	2.05
	δ_C	94.1	52.8	65.2	53.4	70.1	18.8	22.6
	$^3J_{H,H}$	2.5	6.3	3.7	7.3	6.5		
	$^3J_{H,P(\beta)}$	8.4						
Ribose (R)	δ_H	5.97	4.37	4.36	4.28	4.18/4.23		
	δ_C	89.2	74.6	70.5	83.9	65.6		
Uridine (U)	δ_H					5.97	7.95	
	δ_C		167.2		152.6	103.4	142.4	

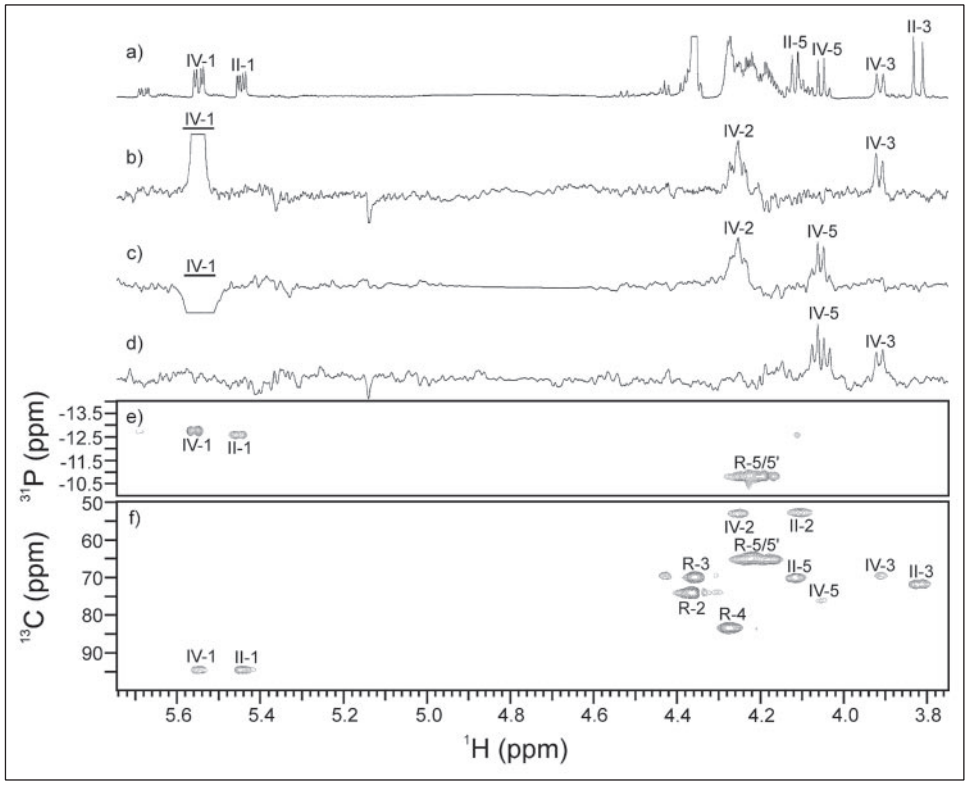

FIGURE 3. **NMR spectroscopy of the reaction products of Cj1293 (II and IV) directly in aqueous reaction buffer (90% H_2O).** The reaction buffer, in addition to II and IV, contained 25 mM $NaPO_4$, pH 7.2, 50 mM NaCl, 0.8 mM pyridoxal phosphate, and 8 mM glutamate. *a*, ^{1}H NMR spectrum. *b*, selective one-dimensional TOCSY (90 ms) of IV H-1. *c*, one-dimensional NOESY (800 ms) of IV H-1. *d*, one-dimensional NOESY (800 ms) of IV H-6. *e*, ^{31}P HSQC spectrum (1 h). *f*, ^{13}C HSQC spectrum (8 h). For selective one-dimensional experiments, excited resonances are underlined. Residue II represents UDP-2-acetamido-2,6-dideoxy-α-D-*xylo*-4-hexulose, residue IV is UDP-2-acetamido-2,6-dideoxy-β-L-*arabino*-4-hexulose, and *R* is ribose.

UDP-α-D-GlcNAc (Fig. 4, *line D, peak III*). Coupling of these two enzymes resulted in loss of both enzymatic activities, resulting in a preparation that was identical to the starting material UDP-α-D-GlcNAc (data not shown), indicating an inhibitory protein-protein interaction. In contrast, no such effect was observed for the Pse enzymes. By uncoupling the two Bac reactions, large scale production of peak III was obtainable (Fig. 4, *line D*).

NMR Analysis of HP0366, Cj1294, and Cj1121c Products—Using one- and two-dimensional homo- and heteronuclear NMR experiments, the purified product of Cj1121c (III) was unambiguously identi-

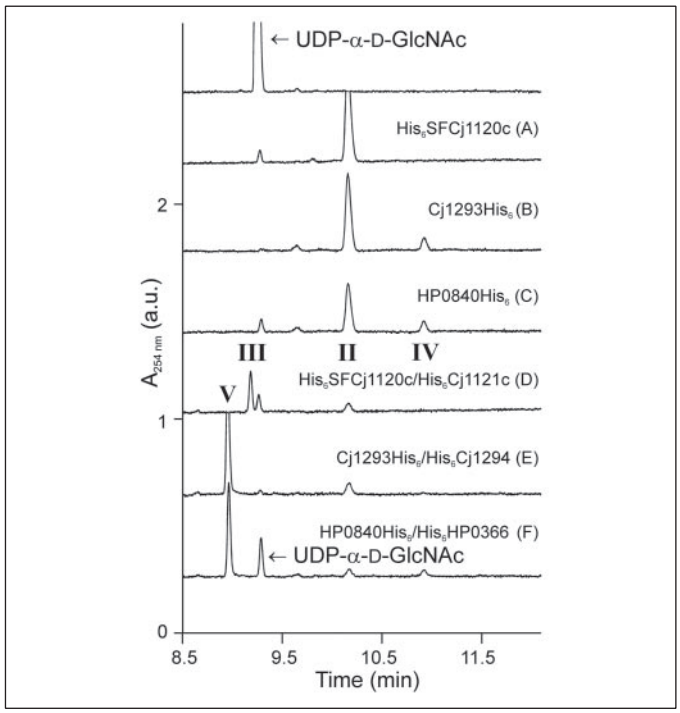

FIGURE 4. **Capillary electrophoresis analysis of the reaction products obtained after catalysis of UDP-α-D-GlcNAc by His_6SFCj1120c (*A*), Cj1293His_6 (*B*), HP0840His_6 (*C*), His_6SFCj1120c/His_6Cj1121c (*D*), Cj1293His_6/His_6Cj1294 (*E*), and HP0840His_6/His_6HP0366 (*F*).** Reactions were performed at 37 °C using 1 mM UDP-α-D-GlcNAc and ~0.3 mg ml^{-1} final enzyme concentration for 3.5 h. Coupled reactions also contained 1 mM PLP and 10 mM L-Glu. *Peak II*, UDP-2-acetamido-2,6-dideoxy-α-D-*xylo*-4-hexulose; *Peak IV*, UDP-2-acetamido-2,6-dideoxy-β-L-*arabino*-4-hexulose; *Peak III*, PgI enzyme product; *Peak V*, flagellar glycosylation enzyme product; *a.u.*, arbitrary units.

fied as UDP-2-acetamido-4-amino-2,4,6-trideoxy-α-D-glucopyranose or UDP-4-amino-4,6-dideoxy-α-D-GlcNAc (Table 3). The ^{13}C and ^{1}H chemical shifts, as well as coupling constants determined for product III, were highly similar to those reported for 2-acetamido-4-amino-2,4,6-trideoxy-α-D-glucopyranose (25, 26) (supplemental Fig. S3).

The purified reaction product of HP0366 and Cj1294 was identified by NMR as UDP-2-acetamido-4-amino-2,4,6-trideoxy-β-L-altropyranose or UDP-4-amino-4,6-dideoxy-β-L-AltNAc (V) (Fig. 5 and Table 3). To verify that unstable intermediates produced by these enzymes were not being lost during purification, the reaction product of HP0366 was analyzed directly in reaction buffer (supplemental Fig. S5). Unlike the HP0840 and Cj1293 *arabino*-4-hexulose products, the UDP-4-amino-4,6-dideoxy-β-L-AltNAc metabolite generated by HP0366 and Cj1294 was considerably more stable and few degradation products were observed (Fig. 5*a*) (supplemental Fig. S4). The selective TOCSY of V H-1 and H-6 permitted the assignment of H-2, H-3, H-4, and H-5, which was confirmed by their coupling constants (Fig. 5, *b* and *c*). The selective NOESY of V H-1 showed NOEs to H-2 and H-5, whereas the ones for H-4 showed NOEs to H-3 and H-5 (Fig. 5, *d* and *e*). Proton-coupling constants and NOEs indicated an altrose configuration for the sugar ring (see below). Chemical shifts were assigned from the ^{13}C HSQC spectrum (Fig. 5*f*).

The pyranose sugar configuration for product V was identified as being β-L-*altro* from NMR data. Altrose pyranose rings are known to be flexible, adopting various conformations. For example, for α-D-altropyransoside, of the possible 38 ring conformations, an equilibrium mixture of 3 stable conformations, $^{4}C_1$, $^{1}C_4$, and $^{0}S_2$ were shown to be present in solution as revealed by quantum mechanical calculations and analysis of proton-coupling constants (27, 28). Consequently, for the β-L-*altro* ring configuration, the $^{1}C_4$, $^{4}C_1$, and $^{2}S_0$ conformers are expected to be the most populated. Analysis of the proton-coupling constants for product V, in a similar manner as was done for α-D-altropyranoside (27), showed that the relative population for the $^{1}C_4$, $^{4}C_1$, and $^{2}S_0$ ring conformations was 60, 25, and 15%, respectively (supplemental Table S1). The NOEs, which are inversely dependent on interproton distances (r) as r^{-6}, were also consistent with several conformations in dynamic equilibrium (supplemental Table S2). For product V, the H-4/H-5 NOE (Fig. 5) can only occur if the $^{4}C_1$ chair is present, because the H-4/H-5 interproton distance is 2.6 Å compared with 3.3 Å in the $^{1}C_4$ chair conformation. The H-6/H-3 NOE was also observed (data not shown), indicative of the presence of the $^{4}C_1$ chair conformation. Further, the coupling constants for the ring protons also changed with temperature, indicative of flexible ring conformations (27). The *altro*-pyranose sugar ring for product V is thus flexible and can adopt multiple chair conformations. For product IV, the coupling constants are indicative of a 45% $^{1}C_4$, 25% $^{4}C_1$ and 30% $^{2}S_0$ distribution. The H-6/H-3 NOE observed for product IV (Fig. 3) is also indicative that the $^{4}C_1$ chair conformation is present, because the H-6/H-3 distance is 1.7 Å as compared with 4.6 Å for the $^{1}C_4$ chair conformation.

Unique Substrate Specificity of HP0366/Cj1294 and Cj1121c Aminotransferases—Further confirmation that the true product of HP0840 or Cj1293 is UDP-2-acetamido-2,6-dideoxy-β-L-*arabino*-4-hexulose is the finding that HP0366 and Cj1294 do not utilize UDP-2-acetamido-2,6-dideoxy-α-D-*xylo*-4-hexulose. Similar to results obtained with *49349* Cj1294 by Obhi and Creuzenet (29) *11168* His_6Cj1294 exclusively uses the initial HP0840/Cj1293 product (Fig. 6*A*), which we have redefined and confirmed here as UDP-2-acetamido-2,6-dideoxy-β-L-*arabino*-4-hexulose. In contrast, His_6Cj1121c exclusively uses UDP-2-acetamido-2,6-dideoxy-α-D-*xylo*-4-hexulose as substrate (Fig. 6*B*). Due to the instability of UDP-2-acetamido-2,6-dideoxy-β-L-*arabino*-4-hexulose, its quantity modestly declined over time in this reaction but not to the significant extent to which UDP-2-acetamido-2,6-dideoxy-α-D-*xylo*-4-hexulose was consumed (Fig. 6*B*). In addition, neither His_6HP0366 nor His_6Cj1294 was able to utilize the product of His_6SFCj1120c (data not shown), further confirming that their substrate is not UDP-2-acetamido-2,6-dideoxy-α-D-*xylo*-4-hexulose.

Kinetic Analysis of Cj1121c and Cj1294—The substrate preparation containing UDP-2-acetamido-2,6-dideoxy-β-L-*arabino*-4-hexulose and UDP-2-acetamido-2,6-dideoxy-α-D-*xylo*-4-hexulose in the ratio of 1:3 was prepared by incubating Cj1293His_6 with UDP-α-D-GlcNAc. This preparation was suitable for studying both Pse and Bac aminotransferases. To note, inhibition due to the complex nature of the substrate material did not appear to be a significant factor, as comparable kinetic values were obtained using Cj1293His_6 filtrates containing a 6:1 ratio of the keto-sugars above, respectively. Both enzymes provided substrate-saturable velocities as determined by Michaelis-Menten kinetic analysis (Fig. 7). Apparent His_6Cj1121c kinetic values of K_m = 0.048 ± 0.0075 mM and k_{cat} = 144 ± 9.5 min^{-1} were calculated using Eadie-Hofstee plots (Fig. 7*A, inset*). Similarly, apparent His_6Cj1294 kinetic values of K_m = 0.052 ± 0.0055 mM and k_{cat} = 4.0 ± 0.21 min^{-1} were obtained using Eadie-Hofstee plots (Fig. 7*B, inset*).

DISCUSSION

We have unequivocally demonstrated that the Pse and 2,4-diacetamido-Bac pathways of *C. jejuni* and *H. pylori* are discrete, and we have defined the initial enzymatic steps of both, stemming from the universal substrate UDP-α-D-GlcNAc. As summarized in Fig. 8, the 2,4-diacetamido-Bac pathway starts with the conversion of UDP-α-D-GlcNAc to UDP-2-acetamido-2,6-dideoxy-α-D-*xylo*-4-hexulose by the C6 dehy-

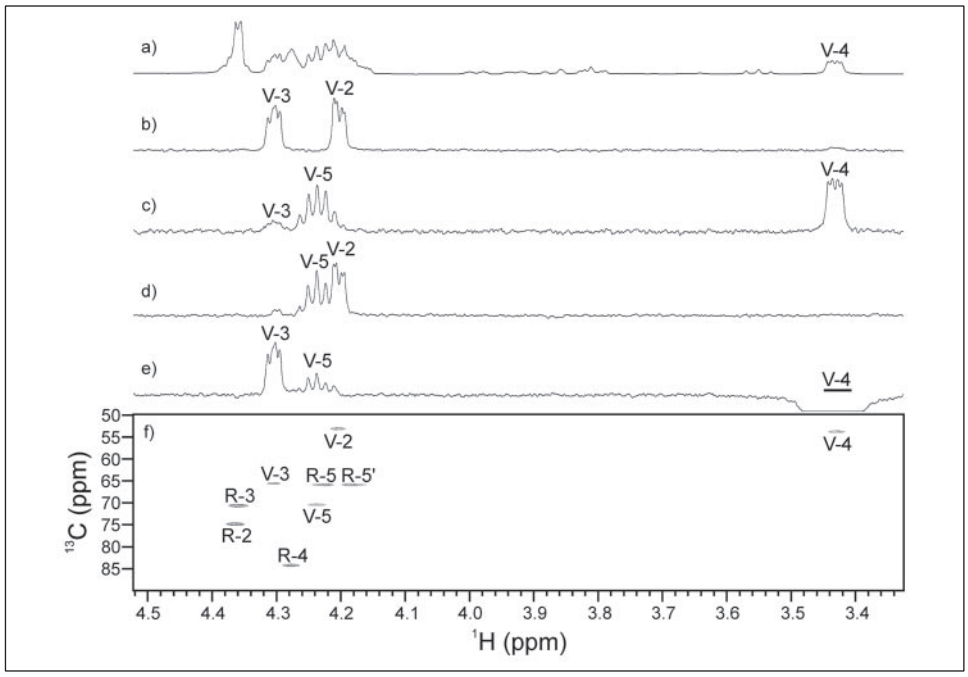

FIGURE 5. **NMR spectroscopy of the purified reaction product of HP0366 (*V*).** *a*, ^{1}H NMR spectrum (nt = 64). *b*, selective one-dimensional TOCSY (90 ms) of V H-1. *c*, one-dimensional TOCSY (90 ms) of V H-6. *d*, one-dimensional NOESY (800 ms) of V H-1. *e*, one-dimensional NOESY (800 ms) of V H-4. *f*, ^{13}C HSQC spectrum ($^{1}J_{C,H}$ = 140 Hz, 15 h). For selective one-dimensional experiments, excited resonances are *underlined*. Residue *V* represents UDP-2-acetamido-4-amino-2,4,6-trideoxy-β-L-altropyranose, and *R* is ribose.

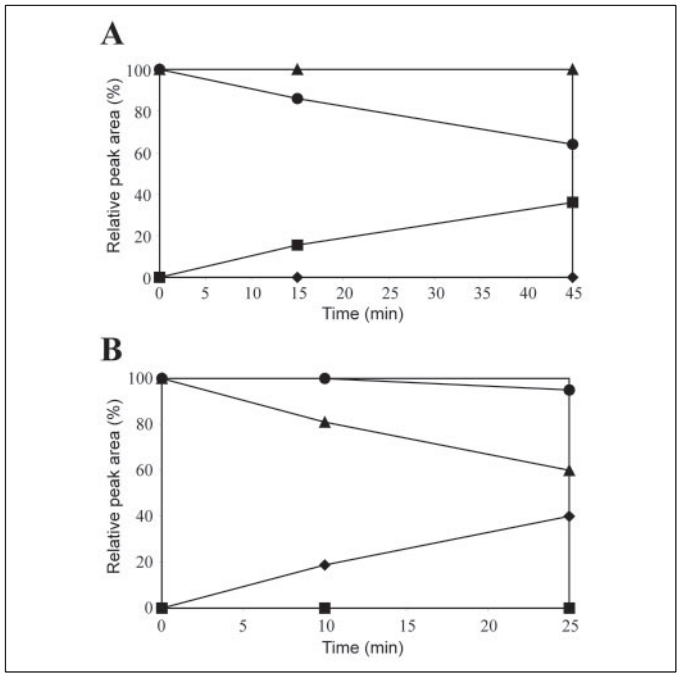

FIGURE 6. **Aminotransferases from the Pse and Bac biosynthetic pathways utilize different substrates.** Cj1294 uses exclusively UDP-2-acetamido-2,6-dideoxy-β-L-*arabino*-4-hexulose as substrate, whereas Cj1121c uses exclusively UDP-2-acetamido-2,6-dideoxy-α-D-*xylo*-4-hexulose. His$_6$Cj1294 (*A*) or His$_6$Cj1121c (*B*) enzyme was incubated with Cj1293His$_6$ filtrate containing both substrates for the times indicated in the presence of 10 mM L-Glu and 1 mM PLP. Samples were then subjected to capillary electrophoresis analysis to obtain the relative peak areas for substrate(s) *versus* product. *Squares*, UDP-4-amino-4,6-dideoxy-β-L-AltNAc product; *diamonds*, UDP-4-amino-4,6-dideoxy-α-D-GlcNAc product; *triangles*, UDP-2-acetamido-2,6-dideoxy-α-D-*xylo*-4-hexulose substrate; *circles*, UDP-2-acetamido-2,6-dideoxy-β-L-*arabino*-4-hexulose substrate.

dratase Cj1120c, followed by C4 aminotransfer of this 4-keto intermediate by Cj1121c to form UDP-4-amino-4,6-dideoxy-α-D-GlcNAc (*steps I→II→III*). The only steps remaining to form the lipid-linked Pgl glycan component 2,4-diacetamido-2,4,6-trideoxy-α-D-glucopyranose (2,4-diacetamido-Bac) are hydrolysis of the phospho-anhydride bond at C1, connecting UMP, and *N*-acetylation at C4. In contrast, the Pse pathway starts with the conversion of UDP-α-D-GlcNAc to UDP-2-acetamido-2,6-dideoxy-β-L-*arabino*-4-hexulose by the C6 dehydratase/C5 epimerase Cj1293, or HP0840, followed by C4 aminotransfer of this 4-keto intermediate by Cj1294, or HP0366, to form UDP-4-amino-4,6-dideoxy-β-L-AltNAc (Fig. 8, *steps I→IV→V*). The final outcome of the C6 dehydratase reaction produces a C4 ketone (30), although the diol forms are depicted in Fig. 8 as the keto group rapidly converts to a diol in aqueous solution. Due to the flexibility of the C5 epimerized pyranose ring, the 4-keto and 4-amino derivatives can adopt various conformations, such as the $^{4}C_{1}$ and $^{1}C_{4}$ chair conformers depicted in Fig. 8. Because the formation of Pse has recently been shown to be catalyzed by a synthase that condenses phosphoenolpyruvate with 2,4-diacetamido-2,4,6-trideoxy-β-L-altropyranose (31), the only remaining steps leading to the formation of this hexose intermediate are, again, hydrolysis of the phosphate ester at C1 and *N*-acetylation at C4.

By using NMR to analyze the products of Cj1293 and HP0840 directly in non-purified aqueous reaction buffer, we have identified unequivocally UDP-2-acetamido-2,6-dideoxy-β-L-*arabino*-4-hexulose (IV) as a key intermediate of the pseudaminic acid pathway. In contrast, previous NMR analysis of the purified or lyophilized reaction products of these two enzymes indicated the presence of only UDP-2-acetamido-2,6-dideoxy-α-D-*xylo*-4-hexulose (II) (data not shown). Although products II and IV were initially present in the aqueous sample, product IV was lost upon purification because of its extreme lability. The heightened sensitivity of the cold probe was also instrumental in characterizing the structure of IV because high quality ^{1}H- and ^{1}H-^{13}C-correlated NMR data could be obtained in comparatively short order. Intramolecular NOEs and $^{3}J_{H,H}$ values measured for IV and V provided evidence indicating that the ring structures of these sugars are in dynamic equilibrium between the $^{4}C_{1}$ and $^{1}C_{4}$ conformations. These findings are in excellent agreement for a sugar with the altrose configuration because the characteristically small energy barrier separating the $^{4}C_{1}$ and $^{1}C_{4}$ conformations of altrose (0.8 to −1.5 kJ/mol) promote pseudorotation (27, 28). Because of its lability and flexible ring, the product of Cj1293 and HP0840 (IV) has been overlooked until very recently and is at the root of the uncertainty and controversy surrounding the bacillosamine

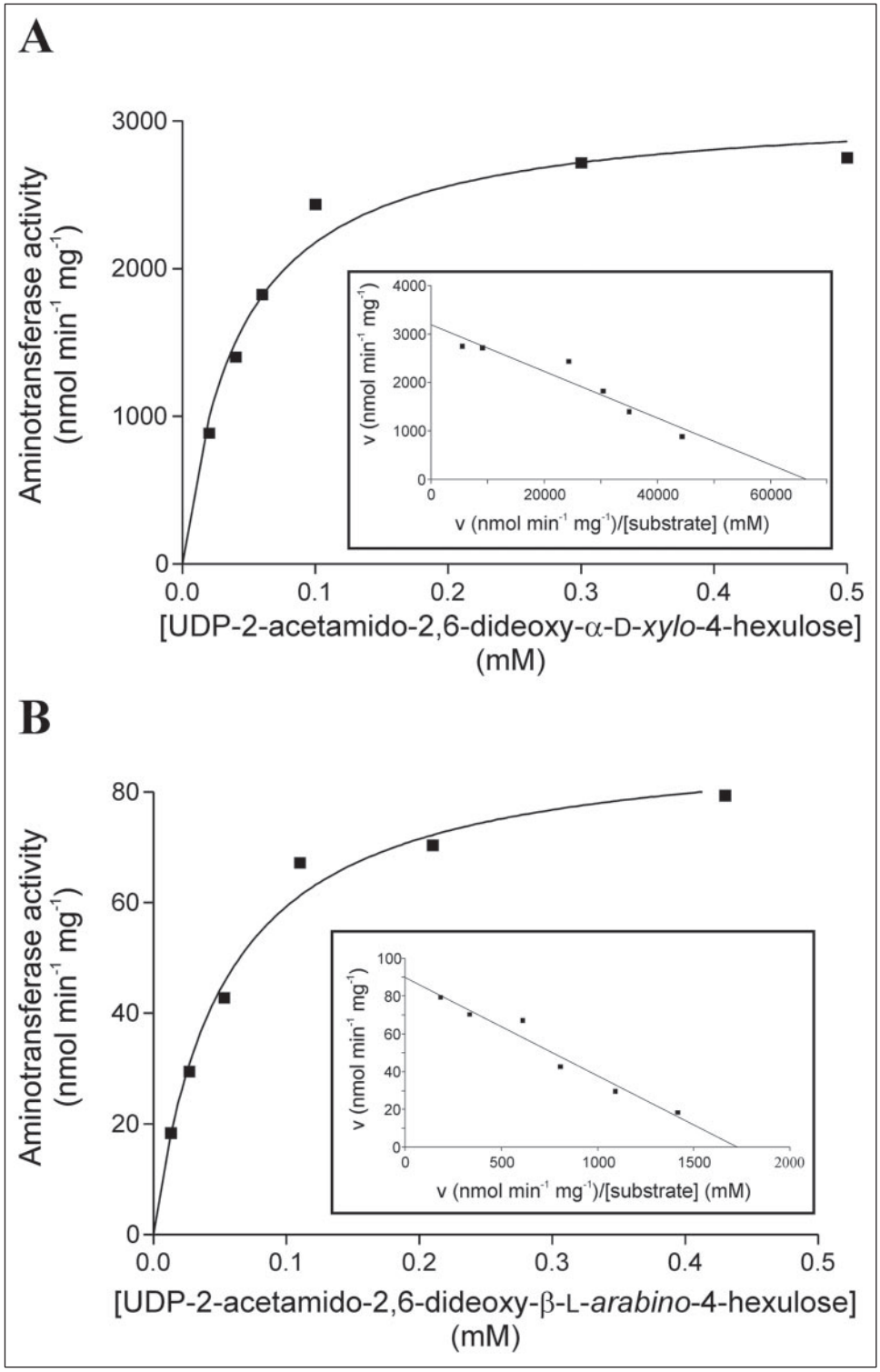

FIGURE 7. **Kinetic analysis of His_6Cj1121c (*A*) and His_6Cj1294 (*B*).** Michaelis-Menten and Eadie-Hofstee (*insets*) analysis of His_6Cj1121c and His_6Cj1294 reactions with the substrate UDP-2-acetamido-2,6-dideoxy-α-D-*xylo*-4-hexulose or the substrate UDP-2-acetamido-2,6-dideoxy-β-L-*arabino*-4-hexulose, respectively. Values represent the average of two independent readings.

and pseudaminic acid pathways in *C. jejuni* and *H. pylori* (21, 22, 29, 32, 33). In addition, recent enzymatic characterization of *49349* Cj1294 suggested that its reaction product (V) was UDP-4-amino-4,6-dideoxy-α-D-GalNAc (29). However, the NMR data reported by Obhi and Creuzenet (29) lack the $J_{4,5}$ coupling constant critical for the *galacto* assignment.

Importantly, to our knowledge, this is the first *in vitro* functional characterization of the *C. jejuni* enzymes Cj1120c and Cj1121c of the novel *N*-linked pathway. Due to anticipated difficulties of expressing the full-length putative membrane protein Cj1120c, we characterized a soluble derivative consisting of residues 130–590, lacking the 4 putative transmembrane regions. This His_6SFCj1120c derivative still retained activity, yet when incubated in a coupled reaction with His_6Cj1121c it was unable to utilize UDP-α-D-GlcNAc. This observation points to an *in vivo* Cj1120c/Cj1121c complex, where its activity could be regulated through secondary interactions, possibly involving the Cj1120c transmembrane region.

HP0840, Cj1293, and Cj1120c belong to a family of enzymes essential for the production of surface-associated virulence factors, including

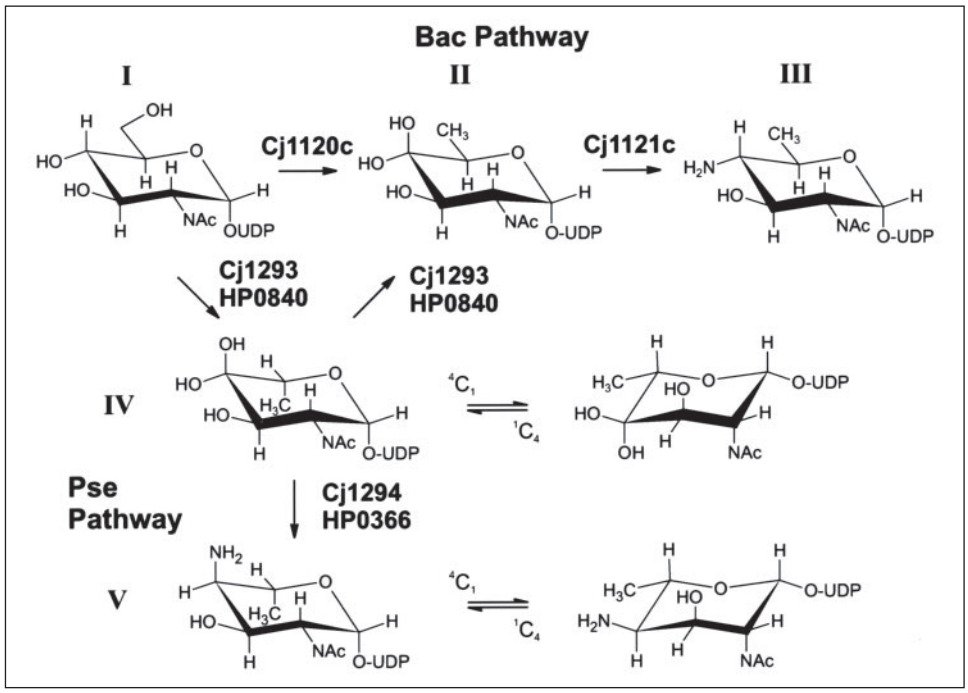

FIGURE 8. **Distinct biosynthetic pathways leading to the production of either Pse or Bac: the initial steps stemming from the universal substrate UDP-α-D-GlcNAc.** *I*, UDP-α-D-GlcNAc; *II*, UDP-2-acetamido-2,6-dideoxy-α-D-*xylo*-4-hexulose; *III*, UDP-4-amino-4,6-dideoxy-α-D-GlcNAc; *IV*, UDP-2-acetamido-2,6-dideoxy-β-L-*arabino*-4-hexulose; *V*, UDP-4-amino-4,6-dideoxy-β-L-AltNAc. The assignment of roman numerals to each compound is consistent with other label designations found throughout the text. Compounds II and IV are drawn as the hydrated forms of their respective keto-sugars.

numerous bacterial pathogens; as such, members of this family have received considerable attention (34–37). Within this family there appear to be two subfamilies, the short soluble enzymes with an SYK catalytic triad of which Cj1293 and HP0840 are members and the large membrane-bound subfamily with an altered SMK catalytic triad, of which Cj1120c and WbpM from *Pseudomonas aeruginosa* are examples. Elegant studies on WbpM, an enzyme essential for B-band LPS biosynthesis, had indicated that this enzyme was a membrane-bound C6 dehydratase/C4 reductase that utilizes UDP-α-D-GlcNAc and produces UDP-6-deoxy-α-D-GlcNAc (UDP-QuiNAc) (23). In this study we have shown the products of Cj1120c and WbpM are in fact UDP-2-acetamido-2,6-dideoxy-α-D-*xylo*-4-hexulose, indicating that these two enzymes are in fact only C6 dehydratases that utilize UDP-α-D-GlcNAc.

In contrast, the two short soluble dehydratase family members examined here, Cj1293 and HP0840, have clearly distinct enzymatic functions, C6 dehydratase/C5 epimerase, which may be a unique distinguishing feature of Pse biosynthetic pathway enzymes or, alternatively, a feature of all members of the short soluble subfamily. Further structural examination by NMR of reaction products from other family members will be required to determine whether these subfamily generalities are legitimate. As depicted in Fig. 8, the C5 epimerization reaction is reversible in that, once the C5 epimer UDP-2-acetamido-2,6-dideoxy-β-L-*arabino*-4-hexulose accumulates, the reaction equilibrium is shifted in favor of the α-D-*xylo* intermediate. This may be a mechanism to shunt non-functional and unstable intermediates into active pathways, such as Pgl glycan production or LPS biosynthesis. In fact, the reversible C5 epimerization reaction shown by HP0840/Cj1293 is the likely reason for its ability to complement a *P. aeruginosa* O5 *wbpM* mutant as well as an *H. pylori wbpB* mutant (32, 34).

The HP0366/Cj1294 and Cj1121c aminotransferase reactions required both PLP and glutamate. We propose that this reaction mechanism is similar to that of *Salmonella typhimurium* ArnB, a PLP-dependent aminotransferase involved in the production of UDP-4-amino-4-deoxy-β-L-arabinose, a key step in lipid A modification (38). Kinetic analysis of the Cj1121c and Cj1294 aminotransferase enzymes did, however, reveal a significant difference. We observed higher overall reaction velocities with the Pgl aminotransferase Cj1121c compared with the Pse aminotransferase Cj1294, although both enzymes exhibited similar binding affinities for their respective substrates (Fig. 7). Because product V (Fig. 8) was predominantly in the $^1C_4$ chair conformation in solution, it is possible that steric hindrance near C4 and C5 due to the C6 methyl group accounts for the lower velocities exhibited by Cj1294. No such steric hindrance would be expected in the $^4C_1$ chair conformations found during the Cj1121c reaction.

In conclusion, this work has demonstrated the inherent complexity of deoxy sugar biosynthetic pathways in bacteria and the difficulty in deciphering these pathways due to lability of certain biosynthetic intermediates. The importance of structural characterization of the biosynthetic precursors should not be underestimated in assigning enzymatic function to proteins that have been identified as functional homologs on the basis of sequence homology alone. As a consequence of the work presented here and to be consistent with the pre-established nomenclature for Cj1293 (33), we propose that the HP0840 (*flaA1*) gene be renamed *pseB* to clearly indicate its role in the Pse biosynthetic pathway. In addition, we propose that the aminotransferase genes Cj1294 and HP0366 be given the designation *pseC* to follow this same nomenclature and to indicate their role in the Pse biosynthetic pathway. Cj1120c and Cj1121c should retain their *pglF* and *pglE* assignment as it has been convincingly shown here that they are involved in the production of 2,4-diacetamido-Bac, a precursor used in assembling the Pgl glycan. Future work combining x-ray crystallographic data with the structural and biochemical data presented in this study will undoubtedly assist in elucidating the reaction mechanisms of these novel dehydratase/epimerases and aminotransferases, as well as in unraveling the structural context important for their substrate specificities.

Acknowledgments—We thank Melissa Schur (Institute for Biological Sciences, National Research Council, Ottawa, ON) for excellent CE technical assistance. We thank Drs. A. Matte and M. Cygler (Biotechnology Research Institute, National Research Council, Montreal, QC) for providing the modified pET15b vector pFO4.

REFERENCES

1. Butzler, J. P., and Skirrow, M. B. (1979) *Clin. Gastroenterol.* **8,** 737–765
2. Dunn, B. E., Cohen, H., and Blaser, M. J. (1997) *Clin. Microbiol. Rev.* **10,** 720–741
3. Parkhill, J., Wren, B. W., Mungall, K., Ketley, J. M., Churcher, C., Basham, D., Chillingworth, T., Davies, R. M., Feltwell, T., Holroyd, S., Jagels, K., Karlyshev, A. V., Moule, S., Pallen, M. J., Penn, C. W., Quail, M. A., Rajandream, M. A., Rutherford, K. M., van Vliet, A. H., Whitehead, S., and Barrell, B. G. (2000) *Nature* **403,** 665–668
4. Fouts, D. E., Mongodin, E. F., Mandrell, R. E., Miller, W. G., Rasko, D. A., Ravel, J., Brinkac, L. M., Deboy, R. T., Parker, C. T., Daugherty, S. C., Dodson, R. J., Durkin, A. S., Madupu, R., Sullivan, S. A., Shetty, J. U., Ayodeji, M. A., Shvartsbeyn, A., Schatz, M. C., Badger, J. H., Fraser, C. M., and Nelson, K. E. (2005) *PloS. Biol.* **3,** e15
5. Tomb, J. F., White, O., Kerlavage, A. R., Clayton, R. A., Sutton, G. G., Fleischmann, R. D., Ketchum, K. A., Klenk, H. P., Gill, S., Dougherty, B. A., Nelson, K., Quackenbush, J., Zhou, L., Kirkness, E. F., Peterson, S., Loftus, B., Richardson, D., Dodson, R., Khalak, H. G., Glodek, A., McKenney, K., Fitzegerald, L. M., Lee, N., Adams, M. D., Hickey, E. K., Berg, D. E., Gocayne, J. D., Utterback, T. R., Peterson, J. D., Kelley, J. M., Cotton, M. D., Weidman, J. M., Fujii, C., Bowman, C., Watthey, L., Wallin, E., Hayes, W. S., Borodovsky, M., Karp, P. D., Smith, H. O., Fraser, C. M., and Venter, J. C. (1997) *Nature* **388,** 539–547
6. Alm, R. A., Ling, L. S., Moir, D. T., King, B. L., Brown, E. D., Doig, P. C., Smith, D. R., Noonan, B., Guild, B. C., deJonge, B. L., Carmel, G., Tummino, P. J., Caruso, A., Uria-Nickelsen, M., Mills, D. M., Ives, C., Gibson, R., Merberg, D., Mills, S. D., Jiang, Q., Taylor, D. E., Vovis, G. F., and Trust, T. J. (1999) *Nature* **397,** 176–180
7. Karlyshev, A. V., Ketley, J. M., and Wren, B. W. (2005) *FEMS Microbiol. Rev.* **29,** 377–390
8. Szymanski, C. M., Logan, S. M., Linton, D., and Wren, B. W. (2003) *Trends Microbiol.* **11,** 233–238
9. Szymanski, C. M., and Wren, B. W. (2005) *Nat. Rev. Microbiol.* **3,** 225–237
10. Logan, S. M., Kelly, J. F., Thibault, P., Ewing, C. P., and Guerry, P. (2002) *Mol. Microbiol.* **46,** 587–597
11. Thibault, P., Logan, S. M., Kelly, J. F., Brisson, J. R., Ewing, C. P., Trust, T. J., and Guerry, P. (2001) *J. Biol. Chem.* **276,** 34862–34870
12. Young, N. M., Brisson, J. R., Kelly, J., Watson, D. C., Tessier, L., Lanthier, P. H., Jarrell, H. C., Cadotte, N., St. Michael, F., Aberg, E., and Szymanski, C. M. (2002) *J. Biol. Chem.* **277,** 42530–42539
13. Wacker, M., Linton, D., Hitchen, P. G., Nita-Lazar, M., Haslam, S. M., North, S. J., Panico, M., Morris, H. R., Dell, A., Wren, B. W., and Aebi, M. (2002) *Science* **298,** 1790–1793
14. Black, R. E., Levine, M. M., Clements, M. L., Hughes, T. P., and Blaser, M. J. (1988) *J. Infect. Dis.* **157,** 472–479
15. Szymanski, C. M., Yao, R., Ewing, C. P., Trust, T. J., and Guerry, P. (1999) *Mol. Microbiol.* **32,** 1022–1030
16. Schirm, M., Soo, E. C., Aubry, A. J., Austin, J., Thibault, P., and Logan, S. M. (2003) *Mol. Microbiol.* **48,** 1579–1592
17. Sambrook, J., Fritch, E. F., and Maniatis, T. (1989) *Molecular Cloning: a Laboratory Manual*, 2nd Ed., Cold Spring Harbor Press, Cold Spring Harbor, New York
18. Brisson, J. R., Sue, S. C., Wu, W. G., McManus, G., Nghia, P. T., and Uhrin, D. (2002) in *NMR Spectroscopy of Glycoconjugates* (Jimenez-Barbero, J., and Peters, T., eds) pp. 59–93, Wiley-VCH, Weinhem, Germany
19. Uhrin, D., and Brisson, J.-R. (2000) in *NMR in Microbiology: Theory and Applications* (Barotin, J. N and Portais, J. C, eds) pp. 165–190, Horizon Scientific Press, Wymonden, UK
20. Berces, A., Whitfield, D. M., and Nukada, T. (2001) *Tetrahedron* **57,** 477–491
21. Creuzenet, C., Schur, M. J., Li, J., Wakarchuk, W. W., and Lam, J. S. (2000) *J. Biol. Chem.* **275,** 34873–34880
22. Creuzenet, C. (2004) *FEBS Lett.* **559,** 136–140
23. Creuzenet, C., and Lam, J. S. (2001) *Mol. Microbiol.* **41,** 1295–1310
24. Kneidinger, B., O'Riordan, K., Li, J., Brisson, J. R., Lee, J. C., and Lam, J. S. (2003) *J. Biol. Chem.* **278,** 3615–3627
25. Maclean, L. L., Vinogradov, E., Crump, E. M., Perry, M. B., and Kay, W. W. (2001) *Eur. J. Biochem.* **268,** 2710–2716
26. Knirel, Y. A., Vinogradov, E. V., Shashkov, A. S., Wilkinson, S. G., Tahara, Y., Dmitriev, B. A., Kochetkov, N. K., Stanislavasky, E. S., and Mashilova, G. M. (1986) *Eur. J. Biochem.* **155,** 659–669
27. Immel, S., Schmitt, G. E., and Lichtenthaler, F. W. (1999) in *Proceedings of the Ninth International Cyclodextrin Symposium*, Santiago de Compostela, Spain, May 31–June 3, 1998 (Torres-Labandeira, J. J., and Vila-Jato, J. L., eds) pp. 41–48, Kluwer Academic Publishers, Dordrecht, Netherlands
28. Ionescu, A. R., Berces, A., Zgierski, M. Z., Whitfield D. M., and Nukada, T. (2005) *J. Phys. Chem. A* **109,** 8096–8105
29. Obhi, R. K., and Creuzenet, C. (2005) *J. Biol. Chem.* **280,** 20902–20908
30. Allard, S. T., Beis, K., Giraud, M., Hegeman, A. D., Gross, J. W., Wilmouth, R. C., Whitfield, C., Graninger, M., Messner, P., Allen, A. G., Maskell, D. J., and Naismith, J. H. (2002) *Structure* **10,** 81–92
31. Chou, W. K., Dick, S., Wakarchuk, W. W., and Tanner, M. E. (2005) *J. Biol. Chem.* **280,** 35922–35928
32. Merkx-Jacques, A., Obhi, R. K., Bethune, G., and Creuzenet, C. (2004) *J. Bacteriol.* **186,** 2253–2265
33. Goon, S., Kelly, J. F., Logan, S. M., Ewing, C. P., and Guerry, P. (2003) *Mol. Microbiol.* **50,** 659–671
34. Burrows, L. L., Urbanic, R. V., and Lam, J. S. (2000) *Infect. Immun.* **68,** 931–936
35. Allen, A., and Maskell, D. (1996) *Mol. Microbiol.* **19,** 37–52
36. Sau, S., and Lee, C. Y. (1996) *J. Bacteriol.* **178,** 2118–2126
37. Skurnik, M., Venho, R., Toivanen, P., and al Hendy, A. (1995) *Mol. Microbiol.* **17,** 575–594
38. Noland, B. W., Newman, J. M., Hendle, J., Badger, J., Christopher, J. A., Tresser, J., Buchanan, M. D., Wright, T. A., Rutter, M. E., Sanderson, W. E., Muller-Dieckmann, H. J., Gajiwala, K. S., and Buchanan, S. G. (2002) *Structure (Camb.)* **10,** 1569–1580

Functional Characterization of Dehydratase/Aminotransferase Pairs from *Helicobacter* and *Campylobacter*: ENZYMES DISTINGUISHING THE PSEUDAMINIC ACID AND BACILLOSAMINE BIOSYNTHETIC PATHWAYS

Ian C. Schoenhofen, David J. McNally, Evgeny Vinogradov, Dennis Whitfield, N. Martin Young, Scott Dick, Warren W. Wakarchuk, Jean-Robert Brisson and Susan M. Logan

J. Biol. Chem. 2006, 281:723-732.
doi: 10.1074/jbc.M511021200 originally published online November 11, 2005
